

Stability Analysis of a Rock Column in Seismic Conditions

M. Barbero · G. Barla

Received: 8 January 2010 / Accepted: 3 April 2010 / Published online: 18 April 2010
© Springer-Verlag 2010

Abstract The stability of a rock column located on a high conglomerate cliff in Roverino, near Ventimiglia, in north-western Italy, has been analysed by continuum and discontinuum modelling, in both static and seismic conditions. The rock column, which is 40 m high and nearly 36,000 m³ in volume, exposes the residential area below the cliff, housing more than 4,000 people, to a high risk level. As the area is located in a seismic region with estimated peak acceleration between 0.24 and 0.28 g, the stability analyses were carried out in both static and seismic conditions. Continuum and discontinuum modelling of the rock mass was carried out by using the finite difference methods and the distinct element methods. It is shown that both methods are effective in describing the modes of instability of the rock column in static conditions. On the contrary, a convincing description of the rock column response induced by earthquake excitation is achieved by discontinuum modelling.

Keywords Slope stability · Numerical modelling · Continuum and discontinuum modelling · Seismic analysis

1 Introduction

In rock slope engineering, the rock mass can be represented by either a continuous or a discontinuous medium. The decision as to the adoption of one representation or the other one is not always straightforward. The uncertainties in rock mass characterisation with respect to the distribution of rock

discontinuities and the assessment of their mechanical properties may call for the use of continuum modelling. However, the existence of major discontinuities associated with joint systems within the rock mass may make it preferable in some cases to use discontinuum modelling.

Continuum modelling is based on the application of either the finite element methods (FEM) or the finite difference methods (FDM). These approaches allow for the incorporation, within the model representing the rock mass, of the major discontinuities through the use of “joint” or “interface” elements with different constitutive laws. Discontinuum modelling, which is usually undertaken with distinct element methods (DEM) or discontinuities deformation analysis (DDA), is particularly appropriate for simulating the rock mass response when both discontinuity systems and the major discontinuities themselves need be taken into account.

The aim of this paper is to examine and to highlight the advantages that can be gained using discontinuum modelling compared to continuum modelling, in the analysis of rock slope stability in seismic areas. Similar problems have been previously studied in the papers by Adachi et al. (1991), Kawamoto et al. (1992), Matsukura (2001), and Hatzor et al. (2004), just to mention a few of them.

The “*Testa di Garibaldi*”, a 40 m high rock column, with an estimated volume of nearly 36,000 m³, standing along a conglomerate cliff, in Roverino, near Ventimiglia, in Italy, is taken as a case study (Figs. 1, 2). Since the floods that hit the north-western regions of Italy in the year 2000, this rock column was a case of special concern until the successful implementation of appropriate stabilisation measures (Barla et al. 2002).

As the study site of interest is located in a region with peak acceleration (PGA) between 0.24 and 0.28 g (return period of 475 years), stability analyses were performed

M. Barbero (✉) · G. Barla
Department of Structural and Geotechnical Engineering,
Politecnico di Torino, Corso Duca Degli Abruzzi 24, Turin, Italy
e-mail: monica.barbero@polito.it



Fig. 1 Overall view of the conglomerate cliff



Fig. 2 Details of the rock column “Testa di Garibaldi”

under both static and seismic conditions. Continuum modelling of the rock mass was carried out with FLAC, and Discontinuum modelling with UDEC. Both codes are developed and up-dated by Itasca Consulting Group, Inc. Minneapolis, MN (USA).

2 Site Characterisation

The Roverino cliff is formed of a conglomerate with rounded calcareous pebbles, ranging in size between 4 and 40 cm, embedded in a sandy–silty matrix that is weakly cemented. This conglomerate is stratified with alternating layers of weak to very weak sandstone and silt (Fig. 3a, b).

The rock column, which contains silt bedding layers of varying thickness, stands on a weak sandstone layer that has been significantly undercut (Fig. 4a, b). The bedding

dips to the SSE with a dip angle ranging between 15 and 20°. The discontinuities in the rock mass are either parallel or nearly orthogonal to the cliff surface.

The rock column is separated from the cliff by a major discontinuity on the NE side, which is not totally persistent and is characterised by a dip direction of 250–260° and a dip angle of 70–85° (Fig. 5a). This discontinuity has undergone a shear displacement of up to 3–4 cm (Fig. 5b), showing that sliding is the most probable type of instability of the rock column.

The morphology of the slope has been strongly affected by erosion processes that have produced cavities and voids of a range of sizes. The combined effects of this erosion, the washing out of sand and silt, and the presence of discontinuities are rock toppling and rock falls. In addition, slides have occurred within the debris cover above the crest of the cliff during heavy rain.

The rock column has been subjected to the following investigations:

Aerial and terrestrial photogrammetry. The geometrical features of the rock column were obtained at a scale 1:1,000 as shown in Fig. 6.

Remote sensing using the analysis of infrared digital imagery. Different zones in the rock mass could be identified having different degree of alteration, density and fracturing based on their colour and thermal capacity. Zones of potential rock falls were inferred.

Geological and discontinuity mapping of the cliff and column.

With the data obtained, a simplified but representative geological cross section of the rock column was obtained as shown in Fig. 7. The rock column is separated from the cliff behind by a major discontinuity (A–B–C) consisting of two distinct portions: A–B, with a dip of 73°, and B–C,

Fig. 3 Photographs showing: **a** the conglomerate; **b** the alternating sequence of conglomerate and silty-sandy layers

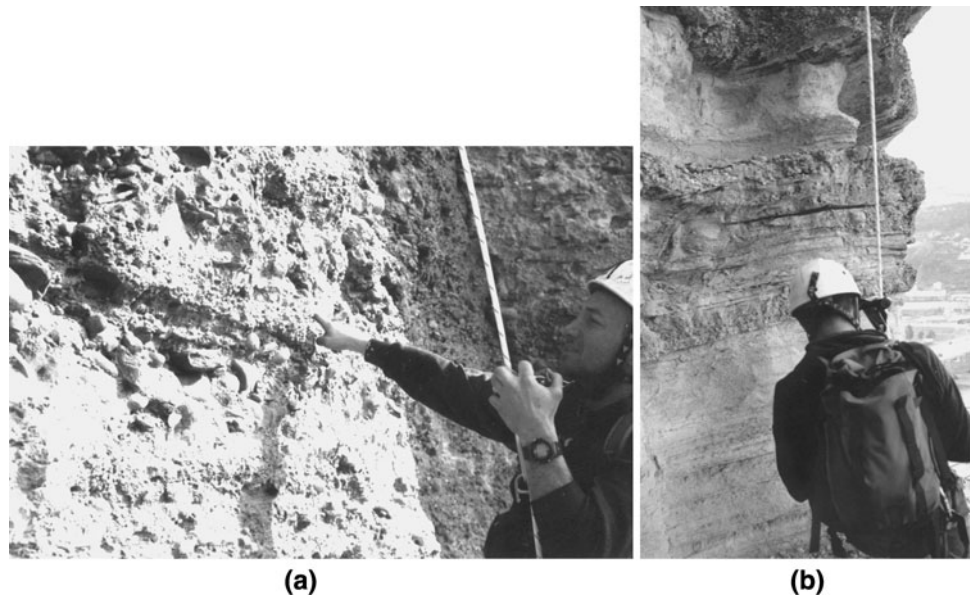
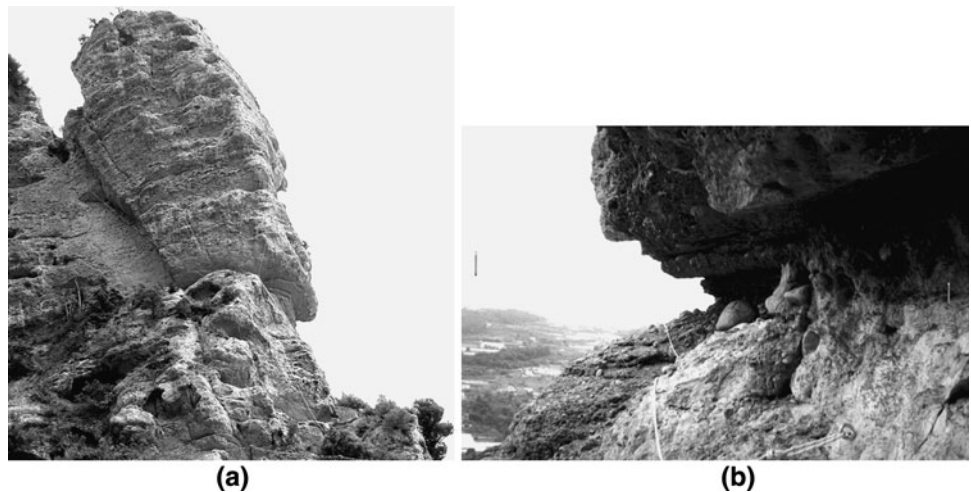


Fig. 4 Close view of the rock column showing: **a** the major discontinuity separating the rock column from the cliff behind; **b** the significant undercut at the bottom of the rock column



with a dip of 61° , both directed out of the slope. Also shown in Fig. 7 is the line C–D, which underlines a possible direction of propagation of the discontinuity.

The mechanical characteristics of the conglomerate (intact rock properties) were obtained with uniaxial compression tests on representative samples (diameter 10 cm, height 20 cm). With the uniaxial compressive strength $\sigma_{ci} = 40$ MPa, a Young's modulus $E = 41$ GPa, and a Poisson's ratio $\nu_i = 0.25$, the m_i Hoek–Brown constant has been taken to be equal to 6, as summarised in Table 1.

The corresponding rock mass parameters (E_d = deformation modulus; c = cohesion; φ = friction angle), were estimated by down-scaling the intact rock properties based on an estimated GSI value of 65 (Hoek and Brown 1997). The mechanical properties of the silty-sandy layers, also given in Table 1, were assessed by back analysis, as described in (Barla et al. 2002).

3 Stability Analyses in Static Conditions

Two-dimensional plane strain analyses were performed in static conditions by taking the cross section of Fig. 7 as representative for both continuum (FDM) and discontinuum (DEM) modelling.

The slope profile was generated in steps by deleting in every step a number of elements as shown in the mesh of Fig. 8, where also shown are the boundary conditions used in static analysis. In addition to the major discontinuity (A–B–C), a number of silty-sandy layers were incorporated in the model including layer 1 at the base level of the rock column (Fig. 7).

The following possible scenarios were considered to simulate the major discontinuity (A–B–C) separating the rock column from the cliff behind and its possible extension along C–D:

Fig. 5 The major discontinuity: **a** view from below; **b** detail showing the movement occurred

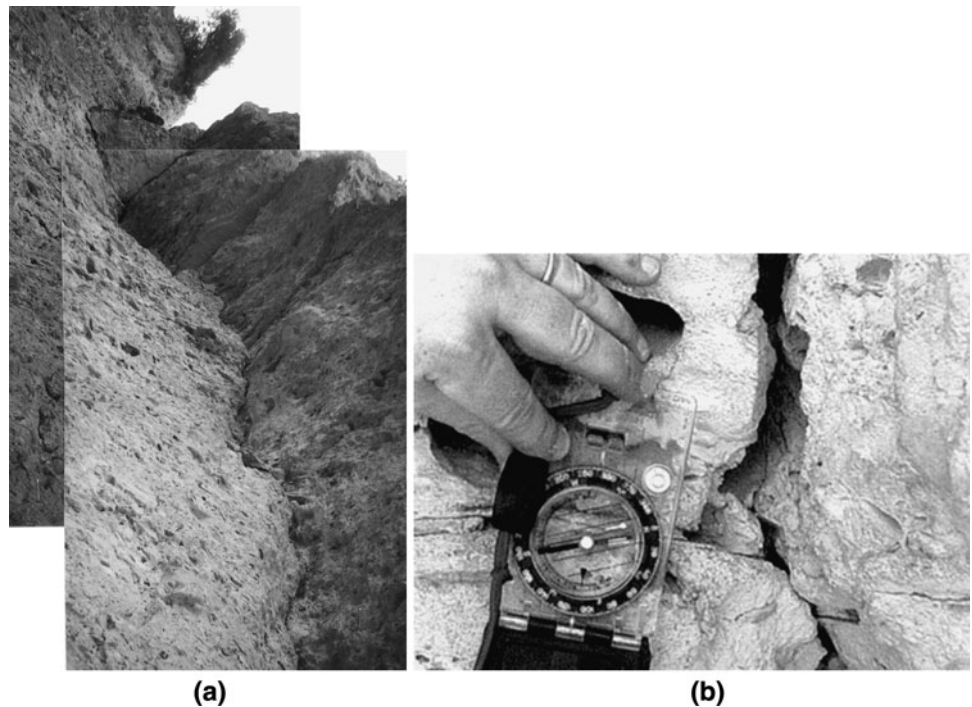
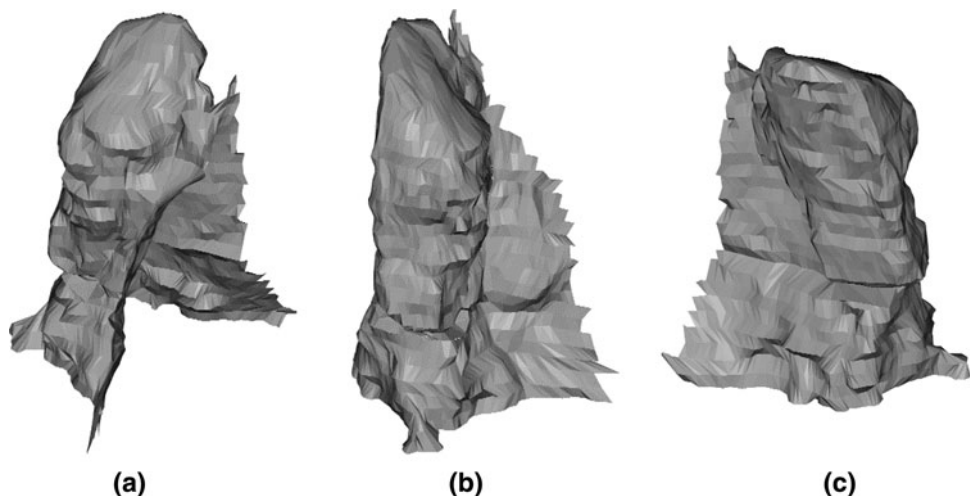


Fig. 6 Three-dimensional representations of the rock column: **a** SE view, **b** SW view, **c** NW view



1. The major discontinuity extends along A–B–C (Fig. 7), which is the condition inferred from the detailed discontinuity mapping;
2. The major discontinuity progressively propagates along line C–D.

Linearly elastic stress–strain behaviour was assumed for the rock mass. An elastic–perfectly plastic Mohr–Coulomb model was adopted for the silty–sandy layers and the major discontinuity A–B–C. In order to determine its shear strength characteristics, parametric analyses were performed for scenario (1), with cohesion (c) and friction angle (φ) along A–B–C being decreased, until a small shear displacement occurred along it. The mechanical parameters given in Table 2 were obtained.

It is shown with both continuum and discontinuum plane strain analyses, in static conditions, that stability of the rock column is attained, if no discontinuity propagation occurs along C–D. Yielding takes place in all the silty–sandy layers (Fig. 9a), showing that their behaviour deeply influences the triggering of instability. Sliding of a few millimetres occurs in the layers and along the discontinuity (lower part of A–B and B–C lines), where also a small opening takes place.

With this condition being reached, the discontinuity propagation was simulated in steps, with a drop of the shear strength parameters from the peak values (rock mass values) down to the residual values (joint values), whenever at a point along C–D the peak shear strength is

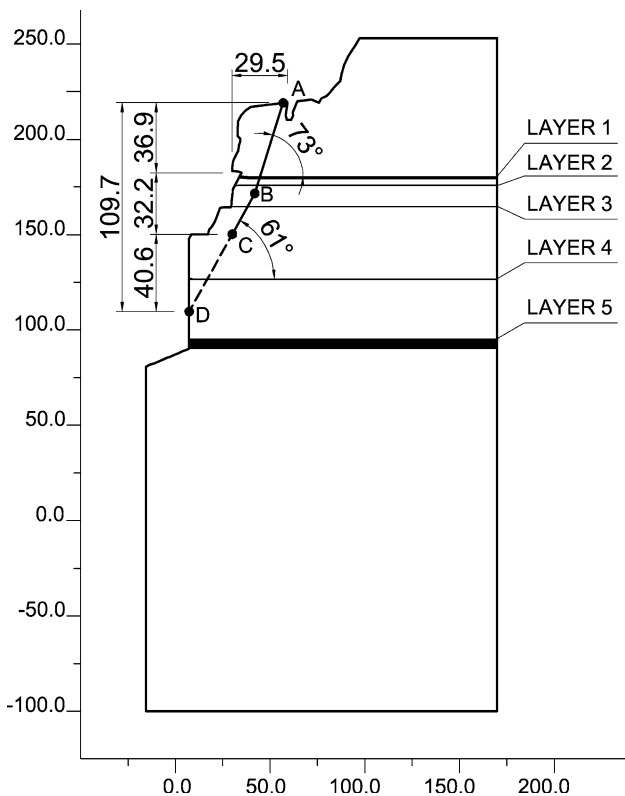


Fig. 7 Geological NW-SE cross section of the rock column showing the silty-sandy layers 1-5 and the major discontinuity A-B-C with line C-D of likely propagation

Table 1 Conglomerate, silty-sandy layers and rock mass mechanical parameters

Parameters		Conglomerate (intact rock)	Silty-sandy layers	Rock mass
Hoek-Brown parameter	m_i	6	-	-
Hoek-Brown parameter	α	0.5	-	-
Uniaxial compressive strength	σ_{ci} (MPa)	40		13
Deformation modulus	E (GPa)	41	1.5	15
Unit weight	γ (kN/m ³)	26	19.6	24
Poisson's ratio	ν	0.25	0.25	0.25
Cohesion	c (MPa)	-	0.10	2.35
Friction angle	φ (°)	-	20	30
Tensile strength	σ_t (MPa)	4.0	-	1.5

reached. It can be observed that propagation of the discontinuity from C to D causes a shear displacement of about 39 cm (Fig. 9b).

The results obtained show that both continuum and discontinuum models are effective in describing the modes of instability of the rock column in static conditions.

4 Stability Analyses in Dynamic Conditions

The Ventimiglia area is characterised by peak ground acceleration (PGA) between 0.24 and 0.28 g (with return period of 475 years). Five destructive earthquakes occurred in the area in the nineteenth century. This means that any realistic study of the stability of the rock column should consider dynamic conditions. Therefore, starting from the results of the previous static analyses, a seismic load history was applied to the model.

No recording of the earthquakes that hit Ventimiglia in the nineteenth century is available. Then, the shock recorded at Assisi (Central Italy), during the seismic event of 26 September 1997 (9:40), was chosen for the purpose of dynamic analysis. This was a bedrock earthquake that had a seismic-tectonic origin similar to the heaviest earthquake, which is known to have occurred in the Ventimiglia area on 23 February 1887, as shown in Fig. 10. The scenario accelerogram, provided by the Italian National Seismic Services, is characterised as follows:

PGA	1.8-2.0 m/s ²
Distance of the epicentre from the seismic station	20 km
Sampling interval	0.01 s
Shock duration	58.85 s

4.1 Numerical Model

A major concern when modelling rock slopes in dynamic conditions is the choice of the mesh geometry and boundary conditions. As shown in Fig. 8, the FDM/FEM model was extended down to the lower horizontal boundary representing the bedrock (100 m below sea level). Two one-dimensional free field columns connected to the side boundaries by means of damping elements were introduced in order to extend the rock mass indefinitely in the horizontal direction (Fig. 11a).

A 2D velocity-time history was applied at the lower nodes of the model. For this purpose, the acceleration records were integrated. The vertical component of the seismic action was maintained unchanged, whereas the horizontal component was projected on the plane of the rock slope section (Fig. 11b, c). The seismic component in the direction perpendicular to the same section was neglected.

Both components of seismic action exhibit most of the energy content in the range 0-6 Hz (Fig. 12a, b). Therefore, in order to delete the contribution of frequencies above 6 Hz, filtering by Butterworth numerical filter was done (Oppenheim et al. 1999). This allowed one to limit the vertical extent of the model and the same mesh could be used for static and dynamic analyses.

Fig. 8 FDM/DEM two-dimensional model adopted for simulation of the rock slope profile in sequential stages: **a** first stage, **b** 10th stage, **c** final configuration

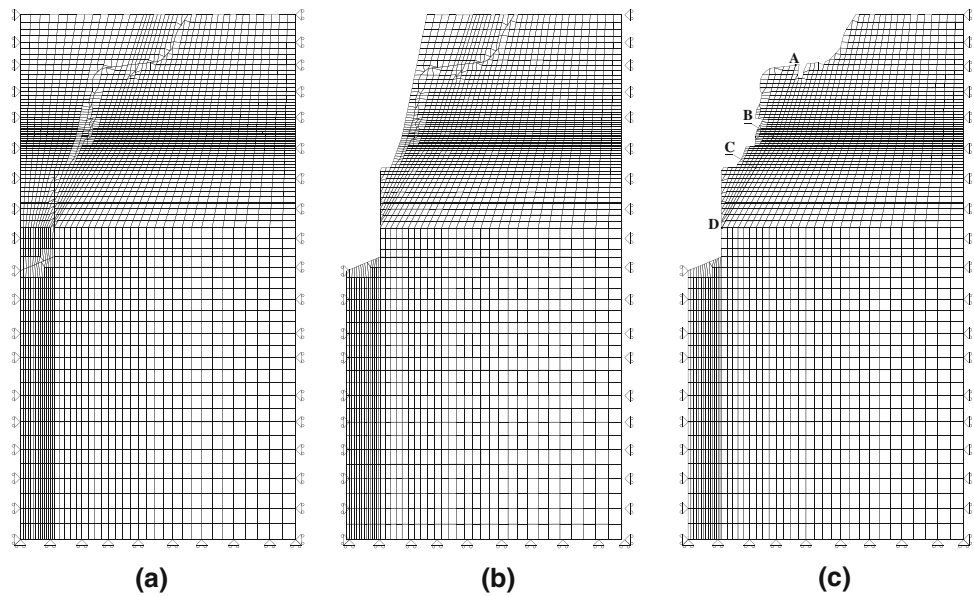


Table 2 Joint mechanical parameters

Parameters		
Normal stiffness	k_n (MPa/m)	2×10^4
Shear stiffness	k_s (MPa/m)	1×10^4
Cohesion	c (MPa)	0.02
Friction angle	φ ($^\circ$)	28
Tensile strength	σ_t (MPa)	0

For correct simulation of wave propagation, the Rayleigh viscous damping formulation was adopted, with the desired damping value (2–5% for geological materials) in the range of the natural frequency of the system, which was determined by performing a numerical analysis with zero damping. The Rayleigh viscous damping constants were

calculated by means of the minimum value of the Rayleigh curve (ζ_{\min}) and the corresponding natural frequency (f_{\min}):

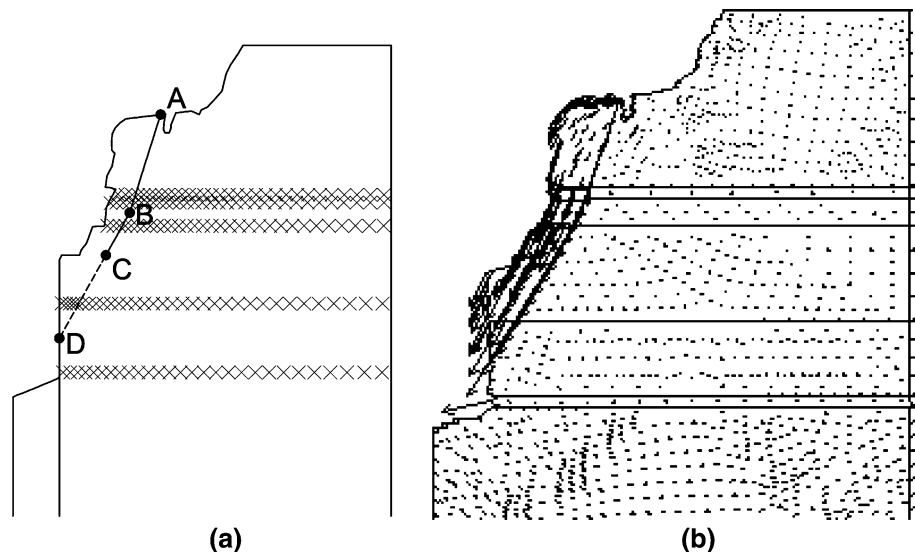
ζ_{\min}	0.03
f_{\min}	1.8 Hz

As shown in Fig. 12c, this choice induces a damping between 3 and 5% in the frequency range from 0.5 up to 6 Hz.

Consistent with the static analyses, the dynamic simulations were performed with the following assumptions:

1. The major discontinuity extends along A–C only;
2. Progressive propagation of the discontinuity is simulated in the C–D direction, with a cohesion drop, from

Fig. 9 Results of static analyses: **a** yielding of the silty-sandy layers; **b** displacements in the rock column with the major discontinuity fully mobilised



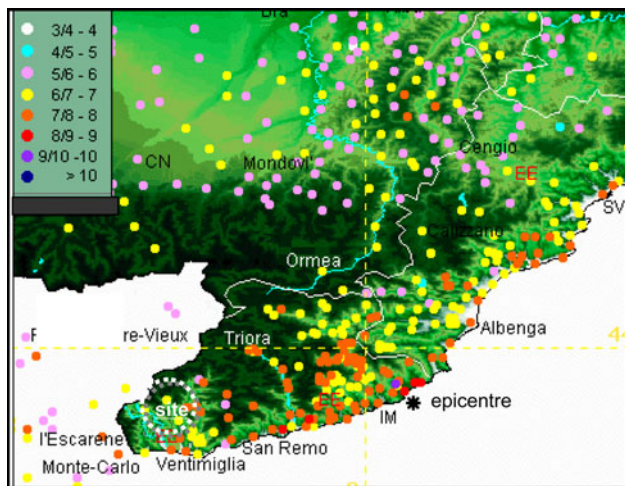


Fig. 10 Intensity of the earthquake occurred on 23rd February 1887 in the vicinity of the site of interest

the rock mass value down to zero, whenever the shear strength is reached;

3. Three different pairs of initial cohesion and tensile strength values along C–D: 100, 50 and 25% of the rock mass value.

As illustrated in Fig. 13, during the analyses, monitoring of the desired variables such as displacement components could be done at the 14 points shown.

4.2 Results of Discontinuum Modelling

The results obtained with discontinuum modelling (UDEC analyses) show in detail the rock column mode of instability. When the seismic action reaches its maximum acceleration value, a stress concentration occurs at point C, which causes the propagation of the major discontinuity along the line C–D.

Between the 10th and the 12th second from the beginning of seismic shaking, all the points along C–D reach the limit equilibrium condition and the downwards movement of the rock column is initiated. In the following seconds, the rock column slides along the discontinuity until, at the 20th second, it collapses as illustrated in Fig. 14.

During the instability phase, the movement of the rock column is rather complex. It oscillates in the horizontal direction, undergoing an alternation of detaching and impacts with the rock mass behind, associated with sliding along the discontinuity. This phenomenon is well illustrated in the acceleration versus time history plot of the monitoring point P3 depicted in Fig. 15. This results in damages of the discontinuity surfaces and stress concentrations at the discontinuity tip, accelerating its propagation outward.

The acceleration of the column reaches its peak after the 10th second from the beginning of the seismic action, both

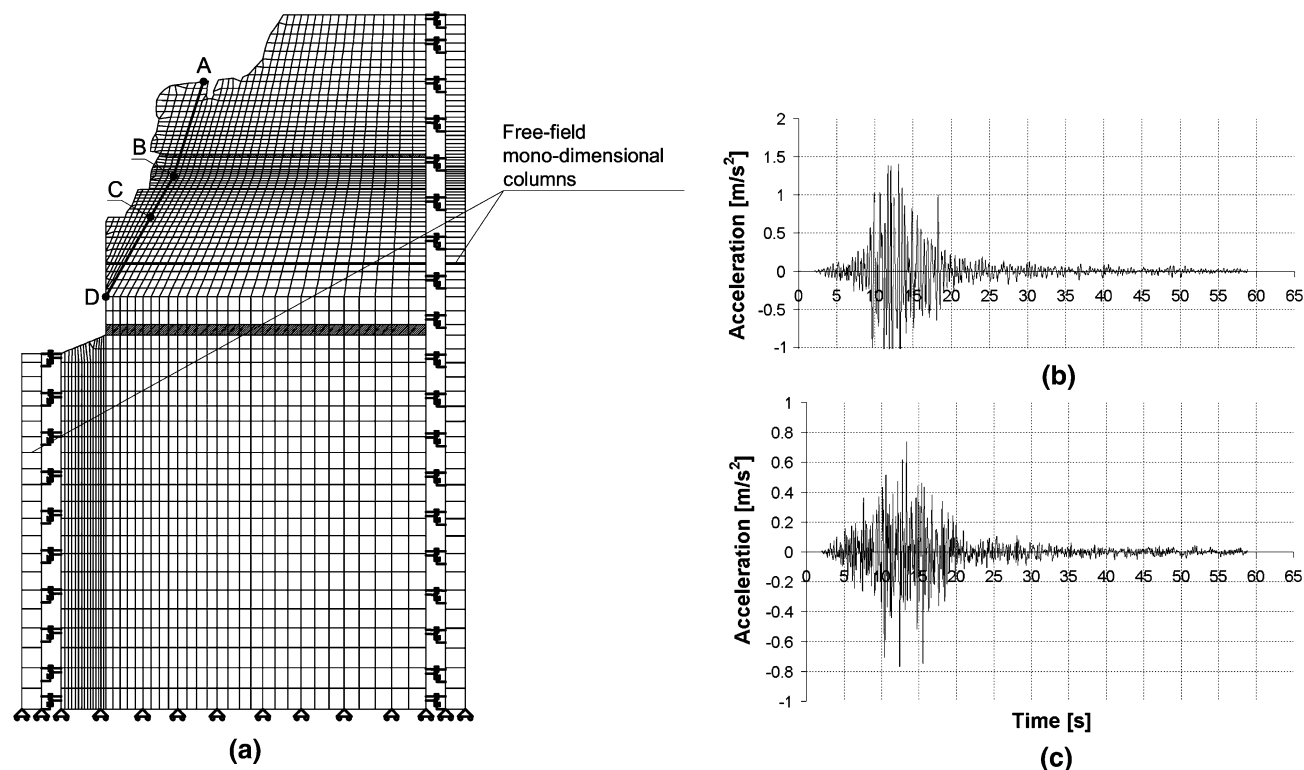


Fig. 11 FDM/DEM two-dimensional model with: **a** boundary conditions for dynamic analyses; **b** horizontal and **c** vertical components of the seismic action

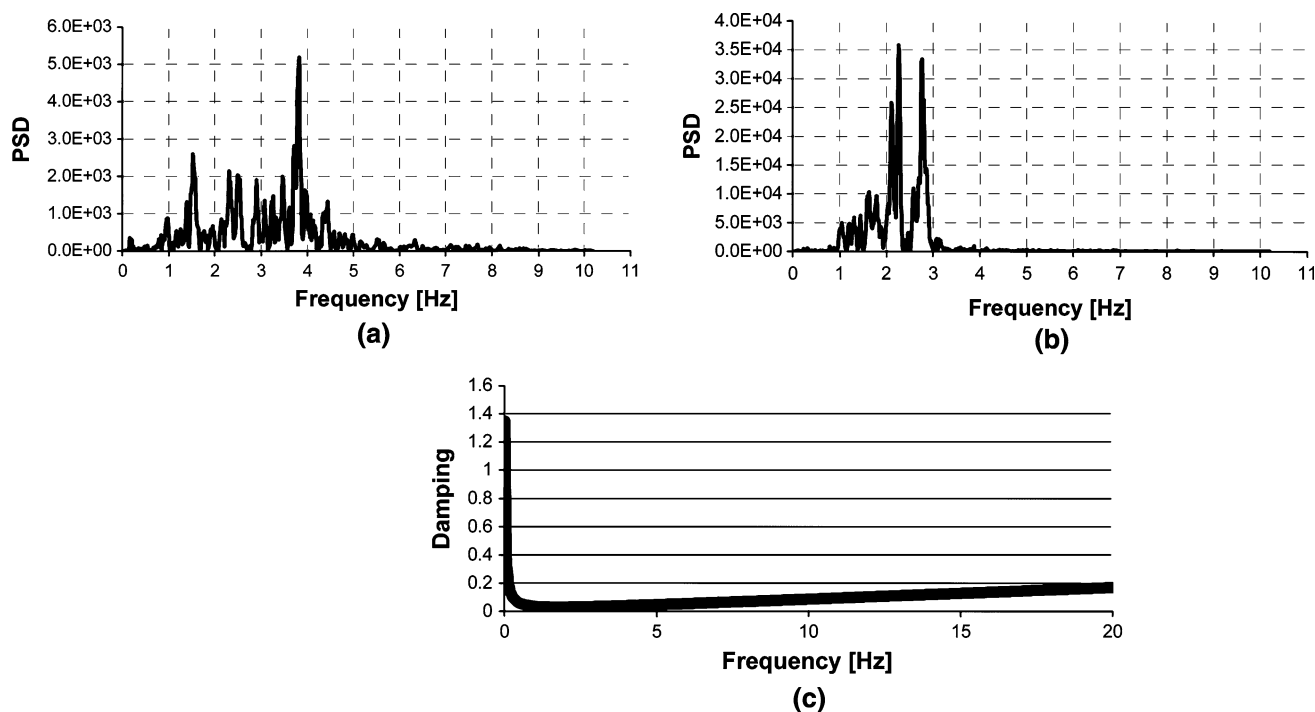


Fig. 12 Power spectrum of the **a** vertical and **b** horizontal components; **c** damping curve

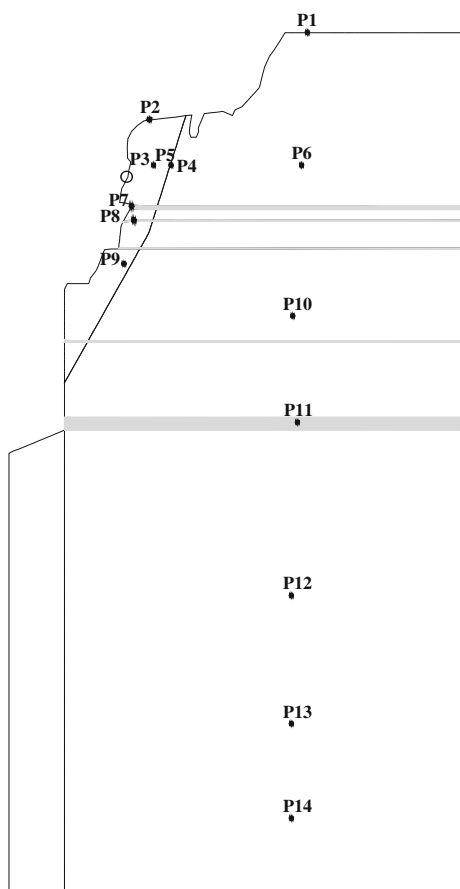


Fig. 13 Monitoring points for plotting the results of dynamic analyses

in the horizontal and vertical directions. A non symmetric pattern of behaviour is clear: an outward horizontal component corresponding to the instants of impact with the rock mass behind; a vertical component that is in the downward direction, leading to progressive fall of the rock column.

During the seismic shock the yielded zones in the silty-sandy layers widen because of the detaching of the rock block and the consequent squeezing out of the same layers. When the block approaches instability, in some points of the layer at the base of the column (layer 1 in Fig. 7) the tensile strength is reached and layer 5 has a tendency to flow outwards (Fig. 16).

It is observed that a decrease of the initial cohesion and tensile strength values along the line C–D does not change the mode of instability. If the initial cohesion and tensile strength values along C–D are 50 or 100% of the rock mass values, block fall takes place anyway, but at a different time. For example, in the first case, the block would fall down after 50 s from the beginning of the seismic action.

The delay in the kinematic evolution is clear when comparing the block displacements obtained for the initial properties along the C–D line of 25 and 50% of the rock mass values. In Table 3, the total displacements of the column are compared after given time intervals. It is observed that the displacements calculated at the same instant are greater if the parameters along C–D are 25% of the rock mass values.

Fig. 14 Development of the rock column instability at 14, 15 s, and up to collapse at 20 s

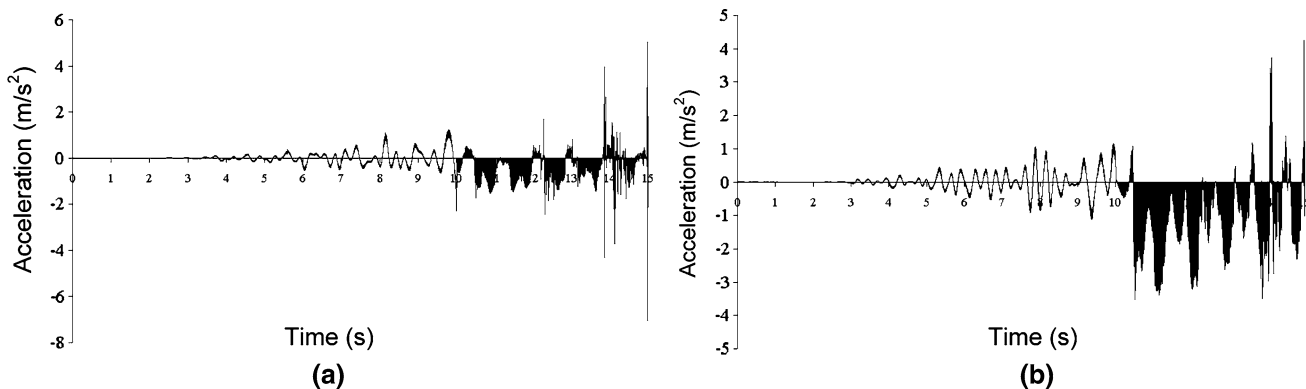
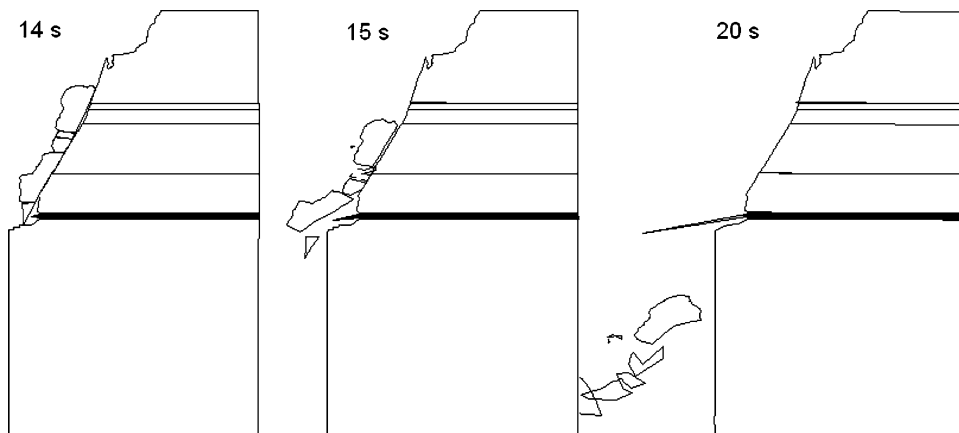


Fig. 15 Acceleration plot at point P3 in the rock column: **a** horizontal and **b** vertical components (point P3 shown in Fig. 13)

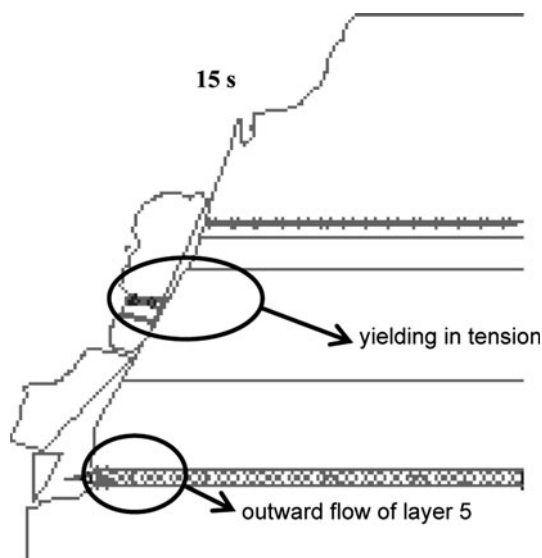


Fig. 16 Yielding in the rock column at the 15th second from the beginning of the seismic action obtained with DEM modelling

Table 3 Total displacements of point 3 at the surface of the rock column, for different strength properties assumed along C–D

Time from the beginning of the seismic action (s)	Cohesion and tensile strength: 25% of the rock mass properties (m)	Cohesion and tensile strength: 50% of the rock mass properties (m)
12	6.22	0.856
13	13.24	1.824
14	25.66	14.67
15	33.77	21.27

cohesion and tensile strength values are 50% of the rock mass values, at the end of the seismic action the block is still stable, showing a maximum horizontal displacement of about 8 cm outwards (Fig. 17).

The earthquake induces the block to oscillate mainly in the horizontal direction with a very small displacement along the vertical. This is a rather improbable movement, as the column has the tendency to move mainly downwards, with a little rotation which induces aperture along the upper part of the discontinuity, as obtained with the static analysis.

4.3 Results of Continuum Modelling

The results obtained with continuum modelling (FLAC analyses) provided somewhat different results. If the initial

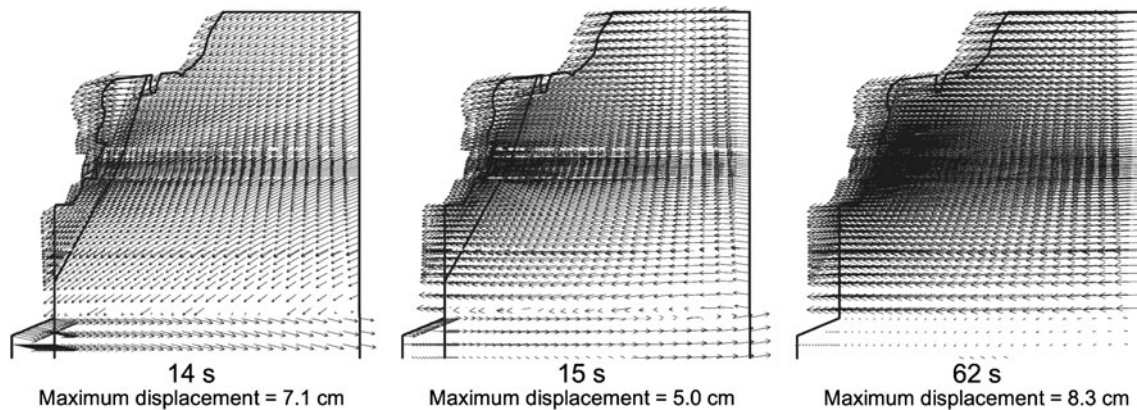


Fig. 17 Rock column displacements at 14, 15 and 62 s from the beginning of the seismic shock computed with the FDM analysis

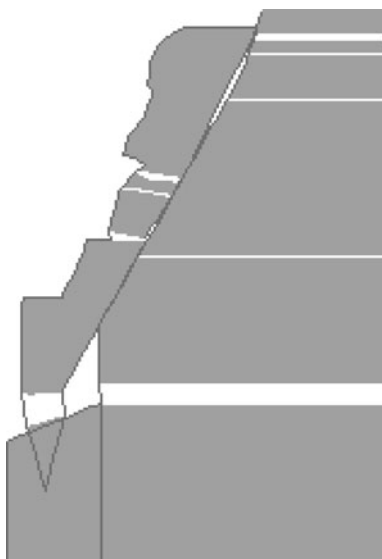


Fig. 18 Rock column configuration at the end of the seismic shock computed with the FDM analysis. Parameters along C–D line equal to the 25% of the rock mass values

This result is due to a significant straining process in layer 5, caused by very high shear stresses, which seem to cause the block movement. In these conditions, no high shear stress concentrations are induced in the C–D direction. As a consequence very few points along the C–D line undergo shear failure, the fracture does not propagate and the block does not fall down.

Only with a reduction of the initial cohesion and tensile strength values along the C–D line to 25% of the rock mass values does the block become unstable. In this case, the mode of instability and the collapse mechanism are very similar to that obtained from the discontinuum analyses, although the block does not fail during the fall, showing a very highly improbable configuration (Fig. 18). In agreement with the DEM results, the yielded points are located in the silty–sandy layers but the reduced resistance

characteristics along C–D allows the downward movement of the column.

5 Conclusions

Numerical analyses were performed using both continuum and discontinuum modelling of the rock mass, with the claim of studying the stability of a rock column located on a high conglomerate cliff in Roverino, near Ventimiglia, in Italy. It was shown that the silty–sandy layers in the rock mass and the discontinuity that separates the rock column from the cliff behind, deeply influence the triggering and development of instability. It was therefore essential to properly simulate the behaviour of both the soft layers and the major discontinuities in the rock mass.

The results obtained from both continuum (FDM) and discontinuum (DEM) analyses have highlighted the on-set of yield in the silty–sandy layers, particularly in the layer at the base of the rock column that makes the global stability conditions critical. In static conditions, if the discontinuity propagates, the block slides along the discontinuity and falls downwards. If the layers and the discontinuity parameters are known and properly represented, both continuum and discontinuum models are appropriate to simulate the response of the cliff.

When the seismic action is taken into account, the modes of behaviour become more complex and only discontinuum modelling seems to correctly simulate the phenomenon under study, in accordance with the results reported by Bhasin and Kaynia (2004) for similar slope stability analyses. It is evidenced that a misunderstanding of the seismic response of the rock column would likely occur using continuum modelling only, as the complex scenarios involving detaching, impacts, oscillations and sliding along the major discontinuity in the rock mass that would drive the column to collapse, are neglected.

References

- Adachi T, Ohnishi Y, Arai K (1991) Investigation of toppling slope failure at route 305 in Japan. In: Balkema (ed) Proceedings 7th international congress on rock mechanics, Aachen. Balkema, Rotterdam, pp 843–846
- Barla G, Papini G, Rabagliati U, Vezzaro V (2002) Stability conditions and remedial works for a high rock cliff near a residential area in north Italy. *Felsbau Rock Soil Eng* 5:188–194
- Bhasin R, Kaynia AM (2004) Static and dynamic simulation of a 700-m high rock slope in western Norway. *Eng Geol* 71:213–226
- Hatzor YH, Arzi AA, Zaslavsky Y, Shapira A (2004) Dynamic stability analysis of jointed rock slopes using the DDA method: King Herod's Palace, Masada, Israel. *Int J Rock Mech Min Sci* 41–5:813–832
- Hoek E, Brown ET (1997) Practical estimates of rock mass strength. *Int J Rock Mech Min Sci* 34:1165–1186
- Kawamoto T, Aydan Ö, Shimizu Y, Kiyama H (1992) An investigation into the failure of a natural rock slope. Proceedings of 6th international symposium landslides, Christchurch 465–470, ed. Balkema, Rotterdam
- Matsukura Y (2001) Rockfall at Toyohama tunnel, Japan, in 1996: effect of notch growth on instability of a coastal cliff. *Bull Eng Geol Environ* 60–4:285–289
- Oppenheim AV, Shafer RV, Buck JR (1999) Discrete-time signal processing. Prentice Hall International